

Article

Dynamic Constitutive Model Analysis of High Parameter Steel Fiber Reinforced Concrete

Dong Luo

Information Technology Centre, Chongqing Jiaotong University, Chongqing 400074, China;
15922957776@163.com

Received: 15 January 2019; Accepted: 21 February 2019; Published: 14 March 2019



Abstract: The traditional Holmquist-Johnson-Cook (HJC) constitutive model does not consider the effect of crack resistance, reinforcement and toughening effect of high parameter steel fiber on original concrete. The causes of the analysis effect of the high parameter reinforced concrete is not obvious. To address this problem, a dynamic constitutive model of high parameter steel fiber reinforced concrete is built in this paper. Based on the static constitutive model built by static force, a dynamic constitutive model is built based on the similarity between static and dynamic stress-strain curve. On this basis, the yield surface equation, state equation, and damage evolution equation of HJC constitutive model are constructed. An improved HJC constitutive model for high parameter steel fiber reinforced concrete is obtained by introducing the modification of the steel fiber reinforced, toughened, and strain rate effects into the HJC constitutive model. Dynamic analysis of high parameter steel fiber reinforced concrete is achieved by using the improved model. Experimental results show that the proposed model is effective in analyzing high parameter concrete and has strong applicability.

Keywords: high parameter; fiber reinforced concrete; dynamic constitutive model; HJC; damage constitutive model; strain rate

1. Introduction

High parameter steel fiber reinforced concrete is a new type of multiphase composite material formed by adding large amounts of randomly distributed steel fibers into the normal concrete. Due to the existence of steel fiber can effectively impede the propagation and expansion of micro cracks in concrete, it can significantly improve the toughness, ductility, and impact resistance of the concrete matrix. The addition of a large amount of steel fiber has a certain effect on the complexity of the concrete [1–5]. Therefore, high parameter steel fiber reinforced concrete belongs to a very complex material. In order to verify the mechanical properties of high parameter steel fiber reinforced concrete under dynamic load [6] and to ensure the safety of engineering design, a series of experimental research work has been carried out by scholars both at home and abroad, and many achievements have been achieved. However, in the constitutive model of high parameter steel fiber reinforced concrete, there is little research on dynamic constitutive model based on impact load. In this paper, the dynamic constitutive model of high parameter steel fiber reinforced concrete is constructed to achieve the numerical analysis of the dynamic response of high parameter steel fiber reinforced concrete structure [7–11].

2. Dynamic Constitutive Model Analysis of High Parameter Steel Fiber Reinforced Concrete

At present, for the numerical simulation of dynamic problems of concrete materials, a more applied model is Holmquist-Johnson-Cook (HJC) model. The model is proposed based on the Johnson-Cook model. It is used to calculate the large deformation of concrete under high pressure

and high strain rate. Due to it can describe the damage, fragmentation and spalling of concrete under high speed impact, it has been widely used in numerical simulation [12]. In this paper, based on the HJC constitutive model, the finite element analysis method for the dynamic constitutive model of high parameter steel fiber concrete is proposed in consideration of crack resistance, reinforcement, and toughening effect of high parameter steel fiber on original concrete.

2.1. Dynamic Constitutive Model Built by Static Force

The dynamic constitutive model built by static force is based on static constitutive model and combined with the similarity between stress-strain curves of static and dynamic forces. The dynamic constitutive model built by static force does not consider the strain rate effect of concrete [13], and the parameters selected are relatively few, which is more convenient in the fitting process. However, the consistency of this kind of constitutive model is slightly deficient. In this paper, the dynamic damage constitutive model is introduced.

For the static constitutive model, the Brooks damage constitutive model is used, as shown in Figure 1.

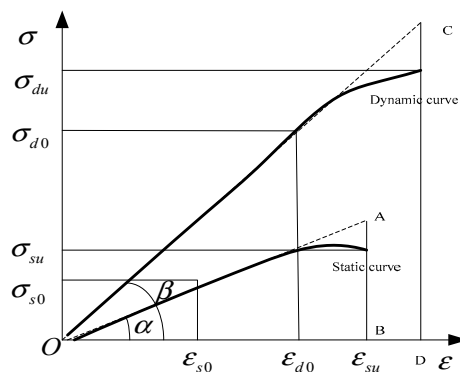


Figure 1. Damage constitutive model.

The mathematical expression is given by:

$$\sigma = \begin{cases} E_s \epsilon_s & \epsilon_s \leq \epsilon_{s0} \\ E_s \epsilon_s (1 - D_s) & \epsilon_s > \epsilon_{s0} \end{cases} \quad (1)$$

E_s is the elastic modulus of initial section of concrete constitutive curve under static condition, ϵ_{s0} is the static damage limit strain, that is, when the strain exceeds the limit, concrete begins to damage [14], D_s is the damage coefficient of concrete under static state. The damage coefficient is expressed as:

$$D_s = \left(\frac{\epsilon_s - \epsilon_{s0}}{k} \right)^n \quad (2)$$

n and k are material constants, which satisfy

$$\begin{cases} n = \frac{\sigma_{su}}{\epsilon_{su}} \left(\frac{\epsilon_{su} - \epsilon_{s0}}{E_s \epsilon_{su} - \sigma_{su}} \right) \\ k = (\epsilon_{su} - \epsilon_{s0}) \left(1 - \frac{\sigma_{su}}{E_s \epsilon_{su}} \right) \end{cases} \quad (3)$$

σ_{su} and ϵ_{su} are peak stress and peak strain of concrete material under static state.

Based on the similarity of the stress-strain curves in the static and dynamic state of the concrete material, the concrete stress-strain curve under static state can be modified by the similar assumption

that the damage evolution process is similar [15]. Then a dynamic damage constitutive model for high parameter steel fiber reinforced concrete is developed:

$$\sigma_d = \begin{cases} E_d \varepsilon_d & \varepsilon_d \leq \varepsilon_{d0} \\ E_d \varepsilon_{ds} (1 - D_d) & \varepsilon_d > \varepsilon_{d0} \end{cases} \quad (4)$$

E_d is the elastic modulus of initial stress-strain curve of concrete under dynamic condition, ε_{d0} is the dynamic damage limit strain [16], D_d is the damage coefficient of concrete under dynamic state.

According to the similarity, the relationship of dynamic D_d and static D_s can be obtained as:

$$\frac{1 - D_d(\varepsilon_d)}{1 - D_s(\varepsilon_s)} = \frac{K_\sigma(\varepsilon, \varepsilon_d)}{K_E(\varepsilon) K_\varepsilon(\varepsilon, \varepsilon_d)} \quad (5)$$

K_σ , K_ε , and K_E are the amplification coefficients of stress, strain, and elastic modulus at any point on the dynamic stress-strain curve of concrete [17]. The amplification coefficient is the ratio of stress (strain and elastic modulus) under dynamic state to the stress (strain and elastic modulus) of the corresponding point under static state.

Assume:

(1) The amplification coefficients of stress and strain of dynamic constitutive curve satisfy the linear relationship.

$$K_\sigma(\varepsilon, \varepsilon_d) = (a + b\varepsilon_d) K_\varepsilon(\varepsilon, \varepsilon_d) \quad (6)$$

(2) The amplification coefficients of strain at any point on the dynamic constitutive curve are the same.

$$K_\varepsilon(\varepsilon, \varepsilon_d) = K_\varepsilon(\varepsilon) \quad (7)$$

Combined with Equations (1) and (4), a and b can be obtained as:

$$\begin{cases} a = K_E(\varepsilon) - \frac{K_\sigma(\varepsilon) - K_E(\varepsilon) K_\varepsilon(\varepsilon)}{K_\varepsilon(\varepsilon_s)} \frac{\varepsilon_{du}}{\varepsilon_{du} - \varepsilon_{d0}} \\ b = \frac{K_\sigma(\varepsilon) - K_E(\varepsilon) K_\varepsilon(\varepsilon)}{K_\varepsilon(\varepsilon) (\varepsilon_{du} - \varepsilon_{d0})} \end{cases} \quad (8)$$

Then the constitutive model with considering strain rate effect is given by:

$$\sigma_d = \begin{cases} K_E(\varepsilon) E_s \varepsilon & \varepsilon \leq \varepsilon_{d0} \\ K_E(\varepsilon) E_s \varepsilon [1 + b(\varepsilon - \varepsilon_{d0})] \left[1 - D_s \frac{\varepsilon}{K_\varepsilon(\varepsilon)} \right] & \varepsilon > \varepsilon_{d0} \end{cases} \quad (9)$$

Chen Jianyun et al. used the same method to propose the dynamic damage evolution law of concrete under dynamic load [18]. The theory is applied to the nonlinear dynamic response analysis of high arch dam, and an ideal finite element analysis result is obtained. It is proved that the application of concrete similarity theory is correct in some fields. Later, some scholars proposed their own theories by using this similar thought [19]. The complete stress-strain equation proposed by Yan Shaohua et al. is directly applied to dynamic situation.

$$\frac{\sigma}{\sigma_{du}} = \frac{\varepsilon/\varepsilon_{du}}{m(\varepsilon/\varepsilon_{du} - 1)^2 + \varepsilon/\varepsilon_{du}} \quad (10)$$

m is material constant.

In this paper, on the basis of static constitutive model built by static force, the HJC constitutive model is improved and the dynamic constitutive model of the high parameter steel fiber reinforced concrete is constructed [20] to achieve the numerical analysis of the dynamic response of high parameter steel fiber reinforced concrete structure.

2.2. Building of HJC Constitutive Model

The HJC model is an elastic-viscoelastic constitutive model containing isotropic damage. The Cauchy stress σ_{ij} in response is divided into hydrostatic stress and deviator stress.

$$\sigma_{ij} = S_{ij} + p_{ij} \quad (11)$$

S_{ij} is the stress deviator, p_{ij} is the Kronecker symbol, p is the hydrostatic pressure in the unit, which is given by:

$$p = \frac{1}{3}\sigma_{kk} \quad (12)$$

The equivalent stress is defined as:

$$\sigma_{eq} = \sqrt{\frac{3}{2}S_{ij}S_{ij}} \quad (13)$$

HJC model includes: Yield surface equation, state equation, and damage evolution equation [21].

(1) Yield surface equation

The yield surface equation of HJC model is given by:

$$\sigma^* = [A(1 - D) + Bp^{*N}] [1 + C \ln(\dot{\epsilon}^*)] \quad (14)$$

$\sigma^* \leq S_{\max}$ is dimensionless equivalent stress, p^* is the dimensionless hydrostatic pressure,

$$\begin{cases} \sigma^* = \sigma_{eq}/f_c \\ p^* = p/f_c \end{cases} \quad (15)$$

S_{\max} is the maximum dimensionless strength of concrete material, f_c is the compressive strength of material under quasistatic state, ϵ^* is the dimensionless strain rate.

$$\dot{\epsilon}^* = \dot{\epsilon}/\dot{\epsilon}_0 \quad (16)$$

$\dot{\epsilon}$ is the equivalent effective strain rate, $\dot{\epsilon}_0 = 1/s$ is the reference strain rate, A is the cohesive coefficient, B is the pressure intensification coefficient, C is the strain rate sensitivity coefficient, N is the pressure intensification index, and D is the damage variable.

(2) State equation

Introduce volume strain μ

$$\mu = \frac{V - V_0}{V_0} = (1 + \epsilon_x)(1 + \epsilon_y)(1 + \epsilon_z) - 1 \approx \epsilon_x + \epsilon_y + \epsilon_z = \epsilon_{kk} \quad (17)$$

The relationship between hydrostatic pressure and volume strain of concrete is described by the piecewise state equation in the HJC model [22], as shown in Figure 2. In the linear elastic stage (OA):

$$\begin{cases} p = K\mu \\ K = \frac{p_c}{\mu_c} \end{cases} \quad (18)$$

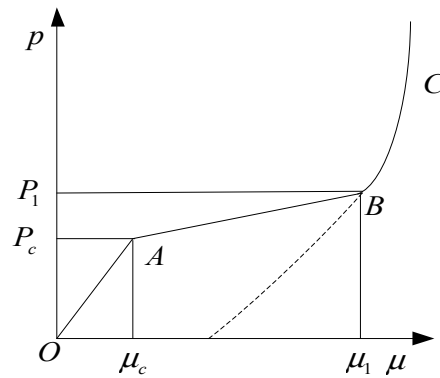


Figure 2. The relationship between hydrostatic pressure and volume strain.

K is the volume modulus of concrete, p_c and μ_c are the pressure and volume strain of concrete during uniaxial compression test.

In the plastic transition stage (AB), the cavity in concrete material is compressed to produce plastic deformation [23]. Under loading:

$$p = p_c + K_1(\mu - \mu_c) \tag{19}$$

$$p_{\max} - p_c = [(1 - F)K + FK_1](\mu_{\max} - \mu) \tag{20}$$

$$F = \frac{\mu_{\max} - \mu_c}{\mu_1 - \mu_c} \tag{21}$$

p_{\max} and μ_{\max} are maximum volume pressure and volume strain before unloading, p_1 and μ_1 are pressure and volume strain of concrete compaction. In this stage, the internal porosity of concrete is gradually eliminated, and the concrete structure is damaged and then begins to produce destructive cracks.

In the complete chamber stage (BC), under loading:

$$p = K_1\bar{\mu} + K_2\bar{\mu}^2 + K_3\bar{\mu}^3 \tag{22}$$

$$\bar{\mu} = (\mu - \mu_1) / (1 + \mu_1) \tag{23}$$

K_1 , K_2 , and K_3 are concrete material constants. Under unloading:

$$p_{\max} - p = K_1(\bar{\mu}_{\max} - \bar{\mu}) \tag{24}$$

(3) Damage evolution equation

In HJC model, the damage is described by the accumulation of equivalent plastic strain and plastic strain [24]. Damage evolution equation is given by:

$$D = \sum \frac{\Delta\varepsilon_p + \Delta\mu_p}{\varepsilon_p^f + \mu_p^f} \tag{25}$$

$\Delta\varepsilon_p$ and $\Delta\mu_p$ are the increments of equivalent plastic strain and plastic volume strain, ε_p^f and μ_p^f are equivalent plastic strain and plastic volumetric strain of concrete under normal pressure,

$$\varepsilon_p^f + \mu_p^f = D_1(p^* + T^*)^{D_2} \geq \varepsilon_{f\min} \tag{26}$$

$T^* = T/f_c$ is the maximum standardized maximum tensile pressure for material, T is the maximum tensile strength of material, $\varepsilon_{f\min}$ is the minimum plastic strain of concrete material when damage, D_1 and D_2 are the constants of damage related to the material of concrete.

2.3. Modified HJC Constitutive Model for High Parameter Steel Fiber Reinforced Concrete

HJC constitutive model is a dynamic constitutive model applicable to concrete with strain rate effect. For high parameter steel fiber reinforced concrete, it has obvious enhancement and toughening effect [25]. Therefore, a modified HJC model is proposed for high parameter steel fiber reinforced concrete, which can reflect the effect of steel fiber on strengthening and toughening of concrete.

(1) Influence of steel fiber on strength

As the equivalent stress and pressure in the modified HJC model are normalized, that is, the ratio of the actual equivalent stress and the static water pressure to the compressive strength f_c under the quasistatic state, the reasonable value of the value of f_c has an important influence on the correctness of the constitutive model. According to the previous analysis [26], the quasistatic compressive strength of high parameter steel fiber reinforced concrete varies with the characteristic parameters of steel fibers. Therefore, the parameter f_c in the constitutive model should reflect the characteristic parameters of steel fiber. Introduce the steel fiber intensification factor K_f :

$$f_c = (1 + K_f)f_{c0} \quad (27)$$

f_{c0} is the quasistatic compressive strength of plain concrete with 0% steel fiber content. For the high parameter steel fiber reinforced concrete, the relationship between K_f and the feature parameters of the steel fiber is obtained from the compressive strength gain equation of the high parameter steel fiber reinforced concrete [27]. The gain equation is substituted into Equation (27), it can be obtained that

$$f_c = \left[1 + 0.038V_f \frac{l_f}{d_f} + 0.17 \left(V_f \frac{l_f}{d_f} \right)^2 - 0.05 \left(V_f \frac{l_f}{d_f} \right)^3 \right] f_{c0} \quad (28)$$

(2) Influence of steel fiber on strain rate effect

In HJC model, the effect of strain rate on strength is expressed as:

$$f(\dot{\varepsilon}^*) = 1 + C \ln(\dot{\varepsilon}^*) \quad (29)$$

the value of strain rate coefficient C is generally less than 0.01, which has low impact on strength and even can be negligible [28]. In this paper, the dynamic intensification factor (DIF) is used as the influence of strain rate on the strength, which is given by:

$$f(\dot{\varepsilon}^*) = a \ln(\dot{\varepsilon}^*) + b \quad (30)$$

The parameters a and b are related to the parameters of the matrix strength and the parameters of the steel fiber

(3) Influence of steel fiber on damage

After the micro cracks appear in the high parameter steel fiber reinforced concrete specimens, the strain release is first used for fiber debonding [29] instead of supporting the continuous expansion of cracks. Therefore, it has delayed the fracture process and played a toughening effect. This process is actually the evolution process of internal damage of concrete. Due to the existence of steel fiber, the damage of high parameter steel fiber reinforced concrete will inevitably decrease compared with plain concrete [30]. Therefore, the relationship between damage factor D and feature parameters of

steel fibers must be established. A large number of experimental researches on concrete and other internal brittle materials show that the internal concrete is not uniform. In which a microelement is taken, its strength obeys a specific statistical law. The intensity of an arbitrary microelement obeys a specific statistical law. Weibull probability distribution is a statistical model which is often adopted. In this paper, assume that the strength of an arbitrary microelement in high parameter steel fiber reinforced concrete is subject to Weibull distribution, which is given by:

$$\phi(\varepsilon) = \frac{m}{\omega} \left(\frac{\varepsilon}{\omega}\right)^{m-1} \exp\left[-\left(\frac{\varepsilon}{\omega}\right)^m\right] \quad (31)$$

ω is the scale parameter, m is the parameter of distribution of defect in material, ε is the strain.

The damage variable D is a measure of the damage degree of the material. The damage intensity is related to the defects contained in each microelement. These defects directly affect the strength of microelements. Therefore, the relationship between the probability density of microelement damages of damage variable D is given by

$$\frac{dD}{d\varepsilon} = \phi(\varepsilon) \quad (32)$$

Substitute Equation (31) into Equation (32) and integral,

$$D = 1 - \exp\left[-\left(\frac{\varepsilon}{\omega}\right)^m\right] \quad (33)$$

The parameters ω and m is fitted, as show in Table 1.

Table 1. Parameter ω and m fitting result.

Fiber Content (%)	CF60				CF80				CF100			
	0	2	4	6	0	2	4	6	0	2	4	6
ω	4	5.01	6.28	9.16	3.82	4.93	6.31	9.06	4.57	5.04	6.17	9.23
m	4.3	3.58	2.31	1.79	4.44	3.66	2.28	1.89	4.63	3.55	2.42	1.73

The regression analysis of the relationship between the parameters ω and m and the feature parameters of steel fibers is carried out respectively. Then

$$\begin{cases} \omega = 4.07 + 0.27V_f \frac{l_f}{d_f} + 0.47\left(V_f \frac{l_f}{d_f}\right)^2 \\ m = 4.43 - 0.92V_f \frac{l_f}{d_f} \end{cases} \quad (34)$$

If the value of the parameter ω is fixed, the larger the parameter m , the larger the damage variable D . There is a linear decreasing relationship between the parameter m and the feature parameter of steel fiber. The results show that the parameter m reflects the brittleness of high parameter steel fiber reinforced concrete (contrary to toughness, the greater the toughness, the smaller the brittleness). From the above analysis, it is known that with the increase of steel fiber content, the toughness of high parameter steel fiber reinforced concrete increases, and the damage degree caused by the same strain is smaller.

(4) Modified HJC model for high parameter steel fiber reinforced concrete

The modification of the reinforcement, toughening, and strain rate effect of the steel fiber is introduced into the HJC constitutive model, and a modified HJC constitutive model for high parameter steel fiber concrete is obtained. The yield surface equation is given by:

$$\sigma^* = (1 + K_f) \left[A(1 - D) + Bp^{*N} \right] \left[a \lg(\dot{\varepsilon}^*) + b \right] \quad (35)$$

The steel fiber intensification factor K_f reflects the intensification effect of steel fiber on concrete. The dynamic intensification factor (the last item in Equation (35)) reflects that the addition of steel fiber weakens the strain rate effect of the matrix concrete. The damage variable D and its evolution equation are defined by Equation (33), which reflects the reduction of the damage degree of the high parameter steel fiber concrete due to the toughening of the steel fiber to the concrete. The state equation still adopts the expression in the HJC model. Through the modified HJC model of high parameter steel fiber reinforced concrete, the dynamic response of high parameter rigid fiber reinforced concrete is accurately analyzed.

3. Experimental Analysis

In order to verify the validity of the proposed model, the proposed model is embedded in the finite element calculation for analysis of the dynamic constitutive model of high parameter steel fiber reinforced concrete. The impact compression experiment of high parameter steel fiber reinforced concrete takes only a few seconds. Only by correlation, the stress-strain change of the specimen can be clearly analyzed during the transient process. Impact analysis of high parameter steel fiber reinforced concrete is obtained with finite element software LS-DYNA. SHPB experimental model for high parameter steel fiber reinforced concrete is built. The theoretical basis of this technique is one-dimensional stress wave theory. The stress-strain relationship of specimen material is derived by measuring the strain on the compression bar. The range of strain rate involved in the SHPB test exactly includes the strain rate at which the flow stress changes with the strain rate. The incident waveform is easy to control and changes the impact velocity and shape of the bullet, which can adjust the incident pulse waveform and thus the waveform acting on the sample. The stress-strain data is extracted and the constitutive curve is drawn out, and then compared with the experimental constitutive curves, so as to verify the correctness of the proposed model. It provides another effective numerical simulation method for the stress of the material in the future. In order to apply the proposed model to the finite element calculation, the second development of the large nonlinear finite element ABAQUS software developed by HKS Company of the United States is implemented to realize the analysis of the proposed model.

The HJC model is a kind of constitutive structure which considers the strain rate effect, damage evolution effect, confining pressure effect and crushing and compaction effect, the HJC model is improved. The influence of hydrostatic pressure and strain rate on the yield strength of concrete is corrected, and the FIF coefficient is introduced into the yield surface equation of HJC model to reflect the influence of steel fiber content on the strength of concrete, so that the HJC model is suitable for steel fiber reinforced concrete. ANN model has obvious advantages in dealing with fuzzy data, random data and nonlinear data. It is especially suitable for systems with large scale, complex structure and unclear information.

3.1. Constitutive Model Unit Test

An 8-node solid element with the side length of 1cm is built in ABAQUS/CAE, as shown in Figure 3. The equal and reverse dynamic load is applied on two symmetrical surfaces, as shown Figure 4.

Since ABAQUS/Explicit has no HJC constitutive model, the test of the proposed model uses another explicit dynamic analysis software LS-dyna. The proposed model is implemented in ABAQUS/Explicit. The same model is built in LS-dyna and calculated by HJC structure model. In order to facilitate comparison, the proposed model is reduced to HJC model of plain concrete.

The stress-strain curves are plotted with the obtained stress-time curve and strain-time curve, as shown in Figure 5.

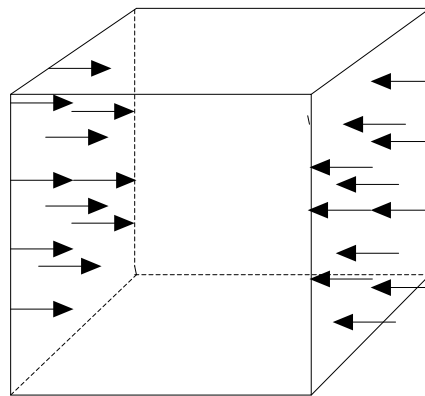


Figure 3. Bi-directional compression model of unit.

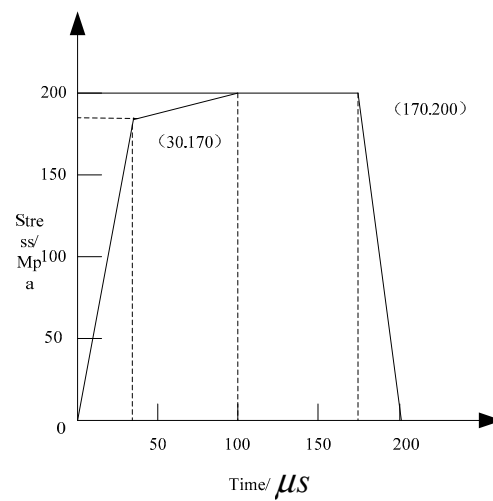


Figure 4. Load time curve.

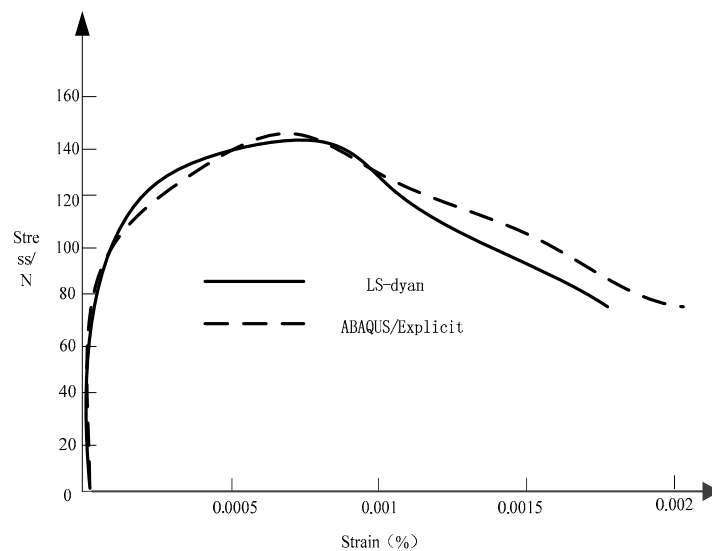


Figure 5. Model improvement results in this paper.

From Figure 5, it can be seen that, with the increase of strain value, the stress value increases linearly in elastic area. After the elastic limit, the stress-strain relationship is transformed into a curve, and a descending segment appears after the peak value. After analyzing the data, it is found that the

decrease of the stress value is due to the accumulation of plastic deformation and the occurrence of damage, so that secant modulus decreases. This stress-strain curve shows that the proposed model can simulate the mechanical behavior of concrete under compression.

The unit shown in Figure 3 is calculated with the proposed model after standard training. The load curve is shown in Figure 4. The matrix strength of the material is 100 MPa and the content of steel fiber is 6%. The input parameters are $f_{c0} = 105$ Mpa, $V_f = 6\%$, and $\frac{l_f}{d_f} = 50$. The results of the calculation are shown in Figure 6. The curve 1 is the curve obtained by eliminating the time variable from the stress-time curve and the strain-time curve of the element. The curve 2 is obtained with the input of the historical information of stress, strain, and strain rate of the element. From Figure 6, it can be seen that the two curves are closer, which shows that the proposed model is feasible and effective in the finite element calculation process.

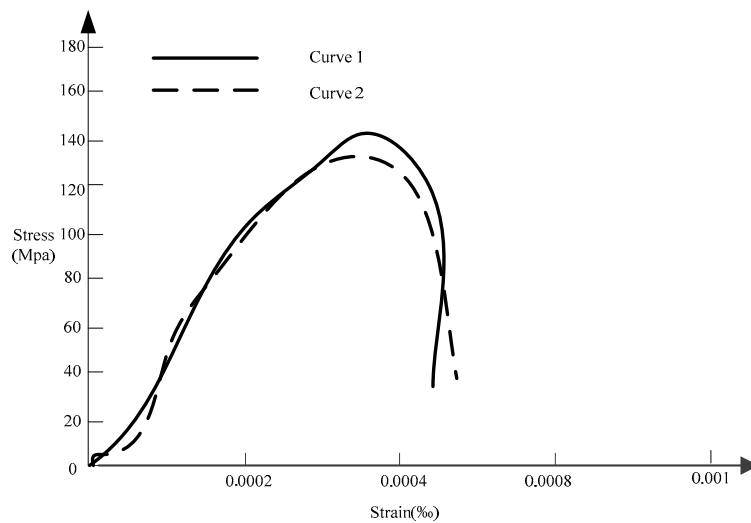


Figure 6. The result of the finite element calculation of the proposed model.

3.2. Response of Simple-Supported Beam Under Impact Load

The high parameter steel fiber reinforced concrete simply-supported beam under impact load is calculated to verify the validity of the proposed model and the corresponding finite element method.

The section size of the high parameter steel fiber reinforced concrete simply-supported beam is 50*50 cm and the span is 4 m. The compressive strength of high parameter steel fiber reinforced concrete is $f_c = 28.8$ Mpa and the tensile strength is $f_t = 3.12$ Mpa. Poisson ratio is $\nu = 0.18$. The uniform load at the top of the simply-supported beam varies with time, as shown in Figures 7 and 8.

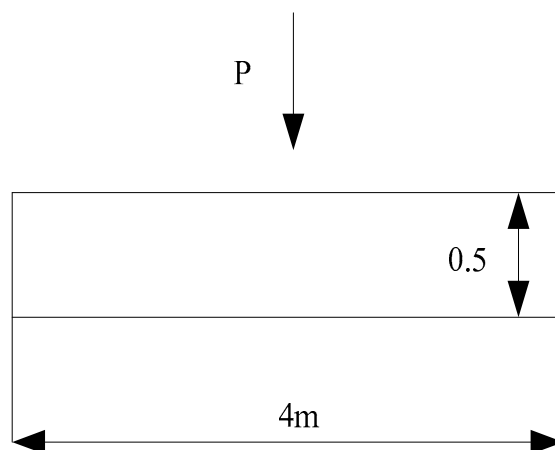


Figure 7. Uniformly distributed load diagram of simple-supported beam.

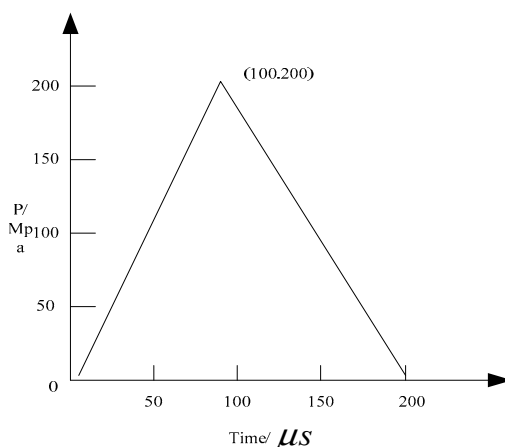


Figure 8. Load time curve.

Figure 9 shows the variation of point deflection in plain concrete simply-supported beam with time. The calculation results of the two proposed models and the ANN model are quite close. In order to investigate the effect of the change of steel fiber on the dynamic response of simply supported beam, the maximum mid-span deflection of steel beams with 0%, 1% and 2% steel fibers was calculated respectively. The results are shown in Table 2.

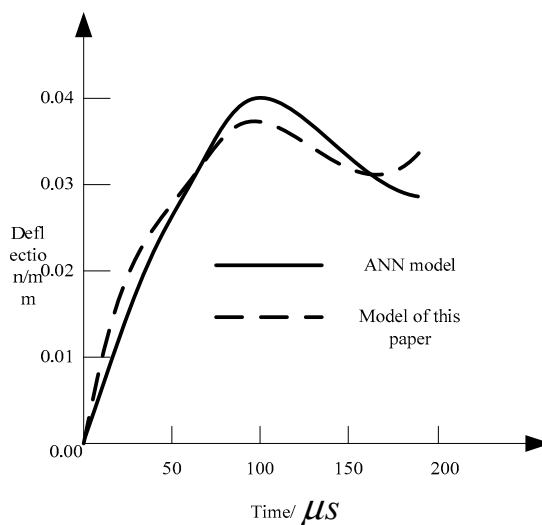


Figure 9. Middle span deflection of plain concrete simple supported beam.

Table 2. The calculation results of the maximum deflection of a simple supported beam span.

Steel Fiber Content (%)	Mid-Span Deflection (mm)		
	HJC Model	Model of This Paper	ANN Model
0	0.025	0.025	0.026
1	—	0.022	0.024
2	—	0.018	0.021

From Table 2, it can be seen that, using the proposed model to calculate plain concrete, it is consistent with the result calculated with HJC model. No matter the high parameter steel fiber concrete adopts the proposed model or the ANN constitutive model, the mid-span deflection decreases when the steel fiber content is increased. It shows the reinforcement effect of steel fiber on concrete. Therefore, the proposed model is reasonable and feasible.

3.3. Numerical Simulation of SHPB Test Process

The SHPB test process of high parameter steel fiber reinforced concrete specimens is simulated by using the proposed model, HJC constitutive model, and ANN constitutive model, respectively. The length of the incident bar and the transmission bar of the model SHPB with the size of $\Phi 100$ mm is 4.5 m and 2.5 m, respectively. The sections of the impact bar and pressure bar are the cylinders with the same material and the length is 0.5 m. The diameter of the specimen is 98 mm, and the length is 50 mm. With the consideration of the symmetry, part of the specimen is modeled. The normal displacement constraint is applied to the nodes of the symmetric plane. The three-dimensional 8-node hexahedral element is used to divide the grid. The mesh of each contact surface is refined, as shown in Figure 10.

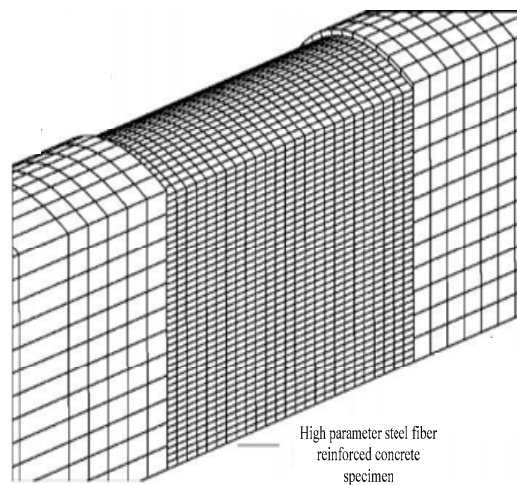


Figure 10. Finite element calculation model.

Waveguide rod material is 45# steel. Linear elastic model is used. The density is $\rho = 7850 \text{ kg/m}^3$, the elastic modulus is $E = 210 \text{ Gpa}$, and the Poisson ratio is $\nu = 0.3$. The strength grade of high parameter steel fiber reinforced concrete specimen is CF100, the steel fiber content is 4%, and the ratio of length to diameter of steel fiber is 50.

The stress-strain relationship of the specimen material is derived by measuring the strain on the compression bar. The element strain in the same position with the strain gauge in the finite element model is selected and the stress-strain relation of the specimen is reconstructed, which is compared with the waveform recorded by the strain gauge, as shown in Figure 11.

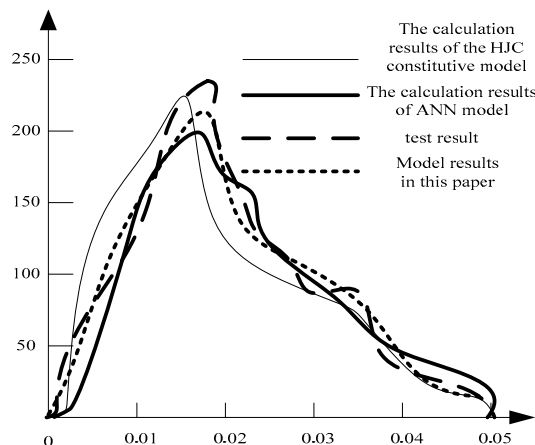


Figure 11. Stress-strain relationship of specimen.

From Figure 11, in the rising stage of stress-strain relationship, the three curves reconstructed by numerical calculation are in good agreement with the experimental curves. However, the results of the HJC constitutive model are different from the experimental results in the initial loading stage. The calculation results of the proposed model and ANN model are basically coincided with the experimental results.

The peak stress of the 4 curves in Figure 11 is not very different. However, the peak strain corresponding to the peak stress is different. This is because the proposed model takes into account the resistance of steel fiber and makes the initial crack strain of high parameter steel fiber concrete increase, so the peak strain should also be increased.

The calculation results of the ANN model are close to the experimental results, in the descending section of the stress-strain relationship, the calculation results of ANN model are close to the test results. The proposed model is close to the ANN model, and the difference between HJC model is larger. The results show that the ANN model contains the strain rate history of the loading path in the training network, and the coverage information is more abundant, so that it can get closer to the test results. It can be seen that the fitting degree between the model and the ANN model is higher, so the proposed model is closer to the experimental results. The proposed model is reasonable and has strong application.

4. Conclusions

The dynamic constitutive model of high parameter steel fiber reinforced concrete is built in this paper. The crack resistance, reinforcement, and toughening effect of high parameter steel fiber on matrix concrete are considered. Based on the calculation results of the high parameter steel fiber reinforced concrete simply-supported beam under impact load, the influence of the change of steel fiber on the dynamic response of simply-supported beam is analyzed. The results show that when the steel fiber content increases, the mid-span deflection decreases. It reflects the reinforcing effect of steel fiber on concrete, and the actual application effect is better.

Funding: This research is supported by National Natural Science Foundation of China (No. 51708068; No. 51778094).

Conflicts of Interest: The authors declare no conflict of interest.

References

1. Anastassova, N.O.; Mavrova, A.T.; Yancheva, D.Y.; Kondeva-Burdina, M.S.; Tzankova, V.I.; Stoyanov, S.S.; Shivachev, B.L.; Nikolova, R.P. Hepatotoxicity and antioxidant activity of some new *N,N'*-disubstituted benzimidazole-2-thiones, radical scavenging mechanism and structureactivity relationship. *Arabian J. Chem.* **2018**, *11*, 353–369. [[CrossRef](#)]
2. Asadi, H.; Bodaghi, M.; Shakeri, M.; Aghdam, M.M. Nonlinear dynamics of SMA-fiber-reinforced composite beams subjected to a primary/secondary-resonance excitation. *Acta Mech.* **2015**, *226*, 437–455. [[CrossRef](#)]
3. Calabrese, A.; Serino, G.; Strano, S.; Terzo, M. Experimental investigation of a low-cost elastomeric anti-seismic device using recycled rubber. *Meccanica* **2015**, *50*, 2201–2218. [[CrossRef](#)]
4. Chagnon, G.; Rebouah, M.; Favier, D. Hyperelastic energy densities for soft biological tissues: A review. *J. Elast.* **2015**, *120*, 129–160. [[CrossRef](#)]
5. Danby, A.M.; Lundin, M.D.; Subramaniam, B. Valorization of grass lignins: Swift and selective recovery of pendant aromatic groups with ozone. *ACS Sustain. Chem. Eng.* **2018**, *6*, 71–76. [[CrossRef](#)]
6. Daniel, I.M.; Cho, J.M.; Werner, B.T.; Fenner, J.S. Characterization and constitutive modeling of composite materials under static and dynamic loading. *AIAA J.* **2015**, *49*, 1658–1664. [[CrossRef](#)]
7. Gao, D.; Chen, G.; Hadi, M.N.S.; Wang, W.; Li, C. Bond-slip behavior and constitutive model between rebar and steel fibre reinforced concrete. *Jianzhu Jiegou Xuebao/J. Build. Struct.* **2015**, *36*, 132–139.
8. Ge, S.; Liu, Z.; Furuta, Y.; Peng, W. Characteristics of activated carbon remove sulfur particles against smog. *Saudi J. Biol. Sci.* **2017**, *24*, 1370–1374. [[CrossRef](#)] [[PubMed](#)]
9. Gholampour, A.; Ozbakkaloglu, T. Finite element analysis of constitutive behavior of FRP-Confined steel fiber reinforced concrete. *Key Eng. Mater.* **2017**, *737*, 511–516. [[CrossRef](#)]

10. Hao, X.; Liu, Y.D. Strength of concrete filled steel tube under fatigue load prediction model simulation analysis. *Comput. Simul.* **2017**, *34*, 361–364.
11. Ju, H.; Kang, S.K.; Lee, D.H.; Hwang, J.-H.; Choi, S.-H.; Oh, Y.-H. Torsional responses of steel fiber-reinforced concrete members. *Compos. Struct.* **2015**, *129*, 143–156. [[CrossRef](#)]
12. Kong, X.; Yong, Q.U.; Zou, D.; Zhang, Y.; Yu, X. Numerical analysis of seismic performance of steel fiber reinforced concrete face rockfill dam. *J. Hydraul. Eng.* **2016**, *47*, 841–849.
13. Li, T.; Fan, D.; Lu, L.; E, J.C.; Zhao, F.; Qi, M.L.; Sun, T.; Fezzaa, K.; Xiao, X.H.; Zhou, X.M.; et al. Dynamic fracture of C/SiC composites under high strain-rate loading: Microstructures and mechanisms. *Carbon* **2015**, *91*, 468–478. [[CrossRef](#)]
14. Lu, X.; Li, Y.; Guan, H.; Yang, M. Progressive collapse analysis of a typical super-tall reinforced concrete frame-core tube building exposed to extreme fires. *Fire Technol.* **2016**, *53*, 1–27. [[CrossRef](#)]
15. Martinez Meza, R.G.; Certucha Barragan, M.T.; Zavala Rivera, P. Removal of iron and manganese from a contaminated effluent using a chelating resin. *Revista Internacional De Contaminacion Ambiental* **2017**, *33*, 55–63.
16. Mehrpay, S.; Jalali, R.S. Strain rate effect in the mesoscopic modeling of high-strength steel fiber-reinforced concrete. *Sci. Iran.* **2017**, *24*, 512–525. [[CrossRef](#)]
17. Mobasher, B.; Yao, Y.; Soranakom, C. Analytical solutions for flexural design of hybrid steel fiber reinforced concrete beams. *Eng. Struct.* **2015**, *100*, 164–177. [[CrossRef](#)]
18. Moreno-Fernandez, S.; Garcés-Rimon, M.; Gonzalez, C.; Uranga, J.A.; López-Miranda, V.; Vera, G.; Miguel, M. Pepsin egg white hydrolysate ameliorates metabolic syndrome in high-fat/high-dextrose fed rats. *Food Funct.* **2018**, *9*, 78–86. [[CrossRef](#)]
19. Orif, M.; El-Maradny, A. Bio-accumulation of polycyclic aromatic hydrocarbons in the grey mangrove (*avicennia marina*) along Arabian gulf, Saudi coast. *Open Chem.* **2018**, *16*, 340–348. [[CrossRef](#)]
20. Othman, H.; Marzouk, H. Applicability of damage plasticity constitutive model for ultra-high performance fibre-reinforced concrete under impact loads. *Int. J. Impact Eng.* **2018**, *114*, 20–31. [[CrossRef](#)]
21. Peng, W.; Li, D.; Zhang, M.; Ge, S.; Mo, B.; Li, S.; Ohkoshi, M. Characteristics of antibacterial molecular activities in poplar wood extractives. *Saudi J. Biol. Sci.* **2017**, *24*, 399–404. [[CrossRef](#)] [[PubMed](#)]
22. Pivoto, D.; Waquil, P.D.; Talamini, E.; Pauletto, C.; Finocchio, S.; Francisco, V.; Corte, D.; de Vargas, M.G. Scientific development of smart farming technologies and their application in Brazil. *Inf. Process. Agric.* **2018**, *5*, 21–32. [[CrossRef](#)]
23. Prem, P.R.; Bharatkumar, B.H.; Murthy, A.R. Influence of curing regime and steel fibres on the mechanical properties of UHPC. *Mag. Concr. Res.* **2015**, *67*, 1–15. [[CrossRef](#)]
24. Spacone, E.; Filippou, F.C.; Taucer, F.F. Fibre beam–column model for non-linear analysis of r/c frames: Part I, formulation. *Earthq. Eng. Struct. Dyn.* **2015**, *25*, 711–725. [[CrossRef](#)]
25. Sucharda, O.; Konecny, P.; Kubosek, J.; Ponikiewski, T.; Done, P. Finite element modelling and identification of the material properties of fibre concrete. *Procedia Eng.* **2015**, *109*, 234–239. [[CrossRef](#)]
26. Tomczyk, L.; Szablewski, T.; Cegielska-Radziejewska, R.; Lewko, L.; Konieczny, P. An assessment of the influence of silver stabilized hydrogen peroxide on the eggshell condition. *Emir. J. Food Agric.* **2018**, *30*, 131–136.
27. Valoroso, N.; Marmo, F.; Sessa, S. A novel shell element for nonlinear pushover analysis of reinforced concrete shear walls. *Bull. Earthq. Eng.* **2015**, *13*, 2367–2388. [[CrossRef](#)]
28. Vu, V.D.; Sheikh, A.H.; Nguyen, G.D.; Shen, L. A kinematically enhanced constitutive model for elastic and inelastic analysis of unidirectional fibre reinforced composite materials. *Int. J. Mech. Sci.* **2017**, *126*, 171–185. [[CrossRef](#)]
29. Wang, J.; Tong, L.; Karihaloo, B.L. A bridging law and its application to the analysis of toughness of carbon nanotube-reinforced composites and pull-out of fibres grafted with nanotubes. *Arch. Appl. Mech.* **2016**, *86*, 361–373. [[CrossRef](#)]
30. Wani, S.A.; Najar, G.R.; Akhter, F. Characterization of available nutrients that influence pear productivity and quality in Jammu & Kashmir, India. *J. Environ. Biol.* **2018**, *39*, 37–41.

